Qu, G. *et al. Géotechnique* [**doi:** 10.1680/geot.8.P.031]

Evaluation of the viscous behaviour of clay using generalised overstress viscoplastic theory

G. QU*, S. D. HINCHBERGER† and K. Y. LO†

In this paper, generalised elastic-viscoplastic (EVP) theory combined with a power law is used to derive simplified equations relating undrained shear strength and preconsolidation pressure to strain rate. An additional equation is derived relating the strain-rate parameter in EVP theory to the secondary compression index. The derived equations are used to evaluate the rate-sensitive and drained creep response of 20 clays reported in the literature. The evaluation shows strong evidence that the rate-sensitivity and time-dependency of clay in compression can be described simultaneously using the generalised EVP theory and power law. In addition, the constitutive parameter governing rate-sensitivity in EVP theory appears to be unique for constant rate-of-strain tests such as undrained triaxial compression and drained oedometer compression as well as stress controlled tests such as drained oedometer creep. To conclude, an approach to select the viscous parameters for clay is provided.

KEYWORDS: clays; shear strength; time dependence

Dans la présente communication, on utilise une théorie élastique-viscoplastique (EVP) généralisée alliée à une loi exponentielle pour dériver des équations simplifiées permettant de calculer les rapports entre la résistance au cisaillement non drainé et la pression de préconsolidation d'une part, et la vitesse de déformation de l'autre. On dérive également une équation supplémentaire mettant en rapport le paramètre de vitesse de déformation dans la théorie EVP et l'indice de compression secondaire. On utilise les équations dérivées pour évaluer la réponse sensible à la vitesse et à la reptation drainée de vingt argiles mentionnées dans la documentation. Cette évaluation apporte des éléments démontrant que la sensibilité à la vitesse et la dépendance temporelle de l'argile sous compression peuvent être décrites simultanément avec la théorie élastique-viscoplastique (EVP) généralisée et la loi exponentielle. En outre, le paramètre constitutif régissant la sensibilité à la vitesse dans la théorie EVP semble être unique pour des essais de vitesse de déformation constante, comme la compression triaxiale non drainée et la compression à l'oedomètre drainé, ainsi que des essais contrôlés par les contraintes, comme la reptation à l'oedomètre drainée. Pour conclure, la communication présente une méthode de sélection des paramètres visqueux pour l'argile.

INTRODUCTION

Suklje (1957) proposed the isotache concept to describe the time-dependent behaviour of clay in one-dimensional oedometer compression. The isotaches were defined as a series of $e - \sigma'_v$ compression curves constructed from tests performed at different constant strain rates. Since then, the concept of isotaches has been extended to yielding in general stress space. For example, Tavenas *et al.* (1978) estimated yield surface isotaches for St. Alban clay in p'–q stress space ($p' = \sigma'_1 + \sigma'_2 + \sigma'_3/3$ and $q = \sigma'_1 - \sigma'_3$). Isotaches were estimated from a series of drained and undrained triaxial compression tests and creep tests. Graham *et al.* (1983) studied the influence of strain rate on Belfast clay using undrained triaxial compression, undrained triaxial extension and one-dimensional (1D) oedometer compression tests and expressed the results in terms of yield surface isotaches plotted in p'–q stress space.

In addition to rate-sensitivity, many natural clays exhibit significant creep or secondary compression at constant effective stress during incremental oedometer tests. Such behaviour is also indicative of the viscous response of clay. Although it is generally recognised that there are similarities between the time-dependent response of clay during undrained and drained compression, so far there has not been a comprehensive analytical study, such as that done in this paper, to generalise the viscous characteristics of clay for these different stress paths (e.g. triaxial compression and oedometer compression).

This paper uses overstress elastic-viscoplastic (EVP) theory, which is commonly used in geomechanics, to examine the viscous response, creep and rate-sensitivity of clays in compression. The main objective is to investigate if a unique set of viscosity parameters can be used to simultaneously describe (i) the rate-sensitivity of clay during drained and undrained compression tests and (ii) the time-dependent behaviour exhibited during secondary compression (Raymond & Wahls, 1976). The secondary objective is to provide guidance for the selection of viscosity parameters for clays.

In the following sections, generalised EVP theory is used to derive theoretical relationships between undrained shear strength and preconsolidation pressure as a function of strain rate. The relationships are expressed in terms of three viscosity parameters called the static yield surface intercept, $\sigma'^{(s)}_{my}$, the fluidity parameter, γ^{vp}, and the rate-sensitivity parameter, α. In addition, a theoretical relationship is also derived from EVP theory relating the rate-sensitivity parameter, α, to the secondary compression index, $C_{\alpha e}$. Then, the measured behaviour of 20 clays (see Table 1) is evaluated during loading along stress paths involving drained K'_o-compression and undrained triaxial compression. Finally, guidance is given for the selection of constitutive parameters for use in EVP constitutive models.

Manuscript received 5 March 2009; revised manuscript accepted 17 November 2009.
Discussion on this paper is welcomed by the editor.
* Trow Associates Inc., Ontario, Canada.
† Department of Civil and Environmental Engineering, The University of Western Ontario, Canada.

Table 1. Geotechnical properties of clays

Clay*	w_N	w_L	I_L	I_P	S_t	C_r	C_c	$C_{\alpha e}$
London clay (England)	23	60	0·08	40	N/A	0·184	0·386	0·036†
Remoulded Boston blue clay (USA)	39·9	45·4	0·77	23·7	N/A	–	–	–
Winnipeg clay (Canada)	60	77	0·62	45	3	$0·1C_c$	$C_{\alpha e}/C_c = 0·018$‡	
Gloucester clay (Canada)	60	52	1·27	30	N/A	0·058	1·495	0·061†
Batiscan clay (Canada)	79·6	43	2·74	21	125	$0·1C_c$	$C_{\alpha e}/C_c = 0·03$‡	
St Alban clay (Canada)	90	50	2·74	23	14	$0·1C_c$	1·72	0·05†
Haney clay (Canada)	–	44	–	18	8	–	–	–
Hong Kong clay	57·4	60	0·92	31·5	–	0·018	0·079	0·0025‡
Drammen clay (Norway)	51	62	0·65	31	–	0·055	0·45	0·016†
St Jean Vianney clay (Canada)	42	36	1·38	16	100	–	–	–
Belfast clay (N. Ireland)	70	90	0·67	60	7·5	$0·1C_c$	$C_{\alpha e}/C_c = 0·05$‡	
Sackville clay (Canada)	61	47	1·74	19	–	0·07	0·646	0·031†
Ska Edeby clay (Sweden)	–	–	–	–	–	$0·1C_c$	$C_{\alpha e}/C_c = 0·05$‡	
Backebol clay (Sweden)	102	99	1·05	65	25	–	–	–
Berthierville clay (Canada)	62	46	1·67	24	–	0·027	0·497	0·027†
St Cesaire clay (Canada)	84·8	70	1·34	43	22	–	–	–
Louiseville clay (Canada)	76·5	70	1·15	43	28	–	–	–
San Francisco Bay mud (USA)	100	93	1·15	48	~7	0·1	0·75	0·05†
Ottawa clay (Canada)	55	31	4	8	>50	–	–	–
Windsor clay (Canada)§	17·2	28	0·23	14	–	0·0165	0·13	0·031

* See Table 2 for references.
† $C_{\alpha e}$ was estimated by the authors from e-log$t$ curves reported in the literature (see Table 2). See Qu (2008) for details.
‡ $C_{\alpha e}$ or $C_{\alpha e}/C_c$ was reported in the literature.
§ See Appendix 2 for Windsor clay.

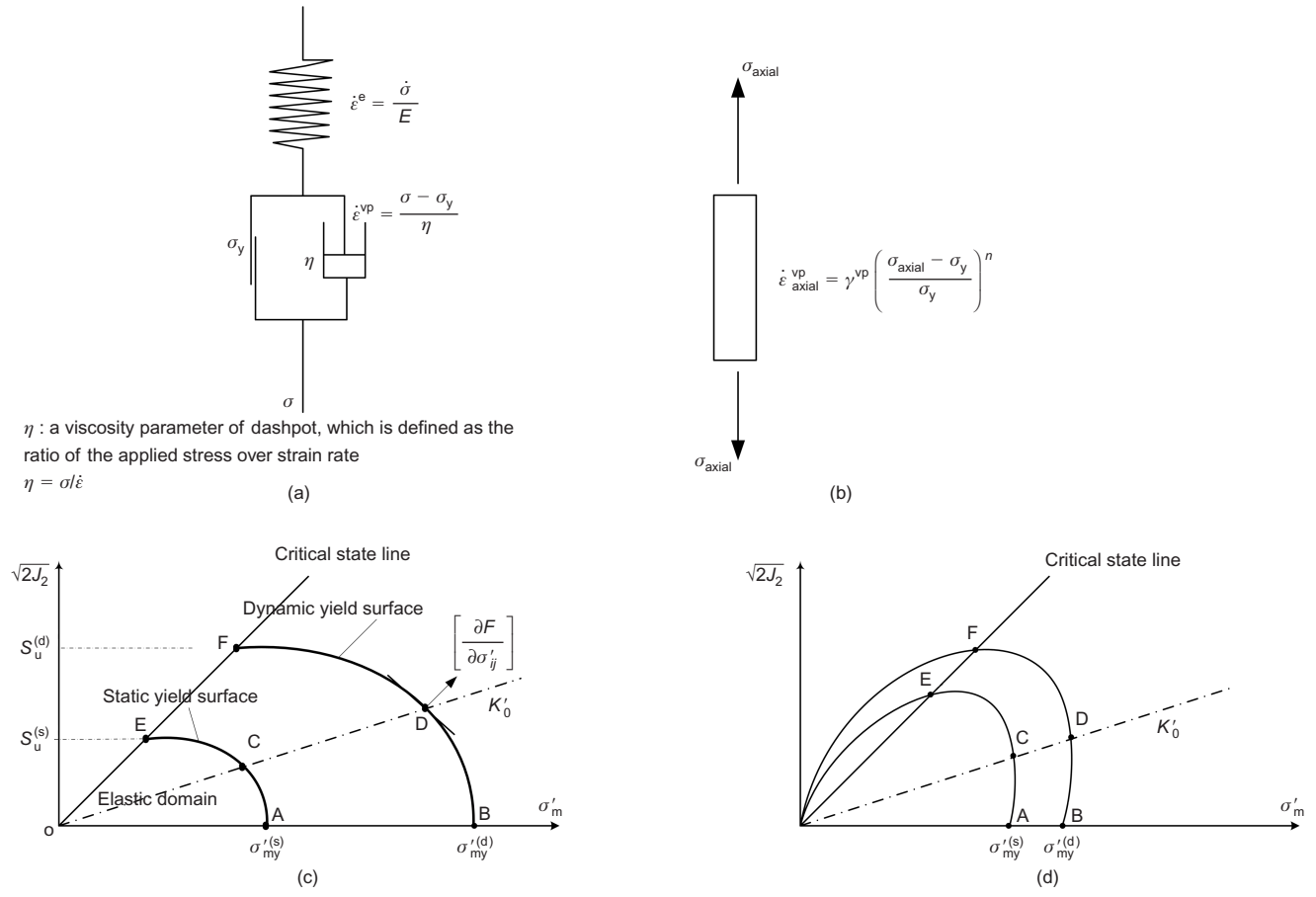

Fig. 1. Illustration of rheologic models for elastic viscoplastic materials

THEORY

Overview of EVP theory

The main characteristics of EVP theory are illustrated in Fig. 1. First, Fig. 1(a) shows a general 1D EVP model comprising a linear elastic spring in series with a plastic slider in parallel with a viscous dashpot. For this type of constitutive model, the strain rate, $\dot{\varepsilon}$, is expressed in terms of elastic, $\dot{\varepsilon}^{\mathrm{e}}$, and viscoplastic, $\dot{\varepsilon}^{\mathrm{vp}}$, components as.

$$\dot{\varepsilon}_{ij} = \dot{\varepsilon}^{\mathrm{e}}_{ij} + \dot{\varepsilon}^{\mathrm{vp}}_{ij} \tag{1}$$

In 1963, Perzyna (1963) proposed an overstress viscoplastic theory to describe the rate-sensitivity of materials at yield during uniaxial tension. For a steel bar in tension (see Fig. 1(b), the viscoplastic axial strain rate from Perzyna (1963) is

$$\dot{\varepsilon}^{\mathrm{vp}}_{\mathrm{a}} = \gamma^{\mathrm{vp}}\langle\phi(F)\rangle\left[\frac{\partial F}{\partial \sigma'_{\mathrm{a}}}\right] = \begin{cases} \gamma^{\mathrm{vp}}\left(\dfrac{\sigma_{\mathrm{a}}-\sigma_{\mathrm{y}}}{\sigma_{\mathrm{y}}}\right)^{n}(1) & \text{for } \sigma_{\mathrm{a}}-\sigma_{\mathrm{y}} > 0 \\ 0 & \sigma_{\mathrm{a}}-\sigma_{\mathrm{y}} \leqslant 0 \end{cases} \tag{2}$$

where $\dot{\varepsilon}^{\mathrm{vp}}_{\mathrm{a}}$ is the axial strain rate, γ^{vp} is the fluidity parameter (min^{-1}), n is a power law exponent, σ_{a} is the rate-dependent axial yield stress and σ_{y} is the yield stress mobilised at a strain rate equal to γ^{vp}. The plastic potential from von Mises failure envelope is unity (1).

Perzyna's (1963) theory of overstress viscoplasticity has been extended to geologic materials by, for example, Hinchberger & Rowe (1998), Desai & Zhang (1987), Katona (1984) and Adachi & Oka (1982). This section utilises the approach adopted by Adachi & Oka (1982) and Hinchberger & Rowe (1998). First, in order to extend Perzyna's (1963) theory to generalised stresses, a suitable yield function must be specified. In this paper, it is assumed that the yield surface is: (a) similar to that illustrated by curve A–C–E–O in Fig. 1(c) or 1(d); (b) a suitable function expressed in terms of the stress invariants σ'_{m}, J_2 and J_3; and (c) a unique curve on the $\sigma'_{\mathrm{m}} - \sqrt{2J_2}$ plane corresponding to compression when normalised by its intercept with the σ'_{m}-axis. In Fig. 1, it should be noted that $\sqrt{2J_2} = \sqrt{2/3}q$. Next, in accordance with overstress viscoplastic theory, the stress state is permitted to exceed the yield surface causing time-dependent plastic strains, which occur at a rate that is proportional to the overstress. Referring to Figs 1(c)–(d), the yield surfaces A–C–E and B–D–F are typically referred to as static and dynamic yield surfaces, respectively. The static yield surface (A–C–E) defines the initial onset of time-dependent viscoplastic behaviour; whereas, the dynamic yield surface (B–D–F) passes through the current stress state and is used to define the overstress and the plastic potential for associated time-dependent plastic flow. The term 'dynamic' yield surface is used since viscoplasticity has typically been viewed as a transient process (see Sheahan *et al.* (1996) and Adachi & Oka (1982)).

From Adachi & Oka (1982) and Hinchberger & Rowe (1998), the EVP constitutive equation for normally consolidated soil is

$$\dot{\varepsilon}_{ij} = \dot{\varepsilon}^{\mathrm{e}}_{ij} + \dot{\varepsilon}^{\mathrm{vp}}_{ij} = C_{ijkl}\dot{\sigma}'_{kl} + \langle\phi(F)\rangle\left[\frac{\partial F}{\partial \sigma'_{ij}}\right] \tag{3}$$

where C_{ijkl} is the elastic compliance tensor and σ'_{kl} is the effective stress tensor. The scalar function, $\phi(F)$, is the flow function, which governs the magnitude of the viscoplastic strain rate, F can be any valid yield surface function from plasticity theory and the plastic potential, $[\partial F/\partial \sigma'_{ij}]$, is a unit vector normal to the dynamic yield surface in $\sigma'_{\mathrm{m}} - \sqrt{2J_2}$ space. In the following sections, simplified theoretical relationships are derived using EVP theory assuming a yield surface function that is consistent with that depicted in Fig. 1(c). However, the following derivations also apply to the yield surface (ACEO) depicted in Fig. 1(d), which is commonly found for clays.

If a power law (Norton, 1929) flow function is used in conjunction with EVP theory, then in terms of generalised stresses the flow function is

$$\phi(F) = \gamma^{\mathrm{vp}}\left(\frac{\sigma'^{(\mathrm{d})}_{\mathrm{my}}}{\sigma'^{(\mathrm{s})}_{\mathrm{my}}}\right)^{n} \tag{4}$$

and

$$\langle\phi(F)\rangle = \begin{cases} \phi(F) & \sigma'^{(\mathrm{d})}_{\mathrm{my}} - \sigma'^{(\mathrm{s})}_{\mathrm{my}} > 0 \\ 0 & \text{for } \sigma'^{(\mathrm{d})}_{\mathrm{my}} - \sigma'^{(\mathrm{s})}_{\mathrm{my}} \leqslant 0 \end{cases}$$

where γ^{vp} is the fluidity parameter and n is the power law exponent. As shown in Fig. 1(c), $\sigma'^{(\mathrm{s})}_{\mathrm{my}}$ is the static yield surface intercept (point A in Fig. 1(c)), $\sigma'^{(\mathrm{d})}_{\mathrm{my}}$ is the dynamic yield surface intercept (point B), and the stress state denoted by point D in Fig. 1(c) is in a state of overstress (e.g. $\sigma'^{(\mathrm{d})}_{\mathrm{my}} > \sigma'^{(\mathrm{s})}_{\mathrm{my}}$). Flow functions similar to equation (4) have been adopted by Adachi & Oka (1982) and Hinchberger & Rowe (1998).

Finally, although there are many different hardening laws, isotropic strain-hardening has been assumed for the following discussions. Expansion or contraction of the static yield surface, $\sigma'^{(\mathrm{s})}_{\mathrm{my}}$, is assumed to be governed by the viscoplastic volumetric strain, $\varepsilon^{\mathrm{vp}}_{\mathrm{vol}}$, as follows

$$\mathrm{d}\sigma'^{(\mathrm{s})}_{\mathrm{my}} = \frac{1+e_0}{\lambda-\kappa}\sigma'^{(\mathrm{s})}_{\mathrm{my}}\mathrm{d}\varepsilon^{\mathrm{vp}}_{\mathrm{vol}} \tag{5}$$

where e_0 is initial void ratio, and λ and κ and are the compression index and recompression index, respectively.

Equations for strain rate controlled testing

Considering constant rate-of-strain (CRSN) isotropic compression, a simplified relationship between the isotropic yield stress, $\sigma'^{(\mathrm{d})}_{\mathrm{my}}$, and axial strain rate, $\dot{\varepsilon}_{\mathrm{a}}$ can be derived explicitly from EVP theory using equations (3)–(5). First, at yield the axial strain rate is

$$\dot{\varepsilon}^{\mathrm{vp}}_{\mathrm{a}} = \left\langle \gamma^{\mathrm{vp}}\left(\frac{\sigma'^{(\mathrm{d})}_{\mathrm{my}}}{\sigma'^{(\mathrm{s})}_{\mathrm{my}}}\right)^{n}\right\rangle\left[\frac{\partial F}{\partial \sigma'_{\mathrm{a}}}\right] = \left\langle \gamma^{\mathrm{vp}}\left(\frac{\sigma'^{(\mathrm{d})}_{\mathrm{my}}}{\sigma'^{(\mathrm{s})}_{\mathrm{my}}}\right)^{n}\right\rangle[1/3] \tag{6}$$

where 1/3 is an estimate of the plastic potential (see Qu, 2008) and is consistent with yield surfaces such as the modified Cam-clay model or the elliptical cap model (see Fig. 1(c)). Taking the logarithm of equation (6) and rearranging gives

$$\log\left(\sigma'^{(\mathrm{d})}_{\mathrm{my}}\right) = \alpha\log\left(\dot{\varepsilon}^{\mathrm{vp}}_{\mathrm{a}}\right) + \left[\log\left(\sigma'^{(\mathrm{s})}_{\mathrm{my}}\right) - \alpha\log\left(\frac{\gamma^{\mathrm{vp}}}{3}\right)\right] \tag{7}$$

where $\alpha = 1/n$ is the rate-sensitivity parameter, n is the power law exponent and $\sigma'^{(\mathrm{d})}_{\mathrm{my}}$ is the dynamic yield surface intercept corresponding to the axial strain rate, $\dot{\varepsilon}^{\mathrm{vp}}_{\mathrm{a}}$.

At yield and failure, the elastic component of strain rate, $\dot{\varepsilon}^{\mathrm{e}}_{\mathrm{a}}$, can be neglected and consequently

$$\log\left(\sigma'^{(d)}_{my}\right) = \alpha \log(\dot{\varepsilon}_a) + \left[\log\left(\sigma'^{(s)}_{my}\right) - \alpha \log\left(\frac{\gamma^{vp}}{3}\right)\right] \quad (8)$$

is sufficiently accurate to interpret the laboratory response in CRSN compression tests. It should be noted that equation (8) does not apply to stress relaxation. As a result, a power law flow function implies a linear relationship between $\log(\sigma'^{(d)}_{my})$ and $\log(\dot{\varepsilon}_a)$, which is depicted by the straight line A–B in Fig. 2(a).

Using a similar approach to that described above, relationships between $\log(S_u^{(d)}) - \log(\dot{\varepsilon}_a)$ and $\log(\sigma_p'^{(d)}) - \log(\dot{\varepsilon}_a)$ can be derived, where $S_u^{(d)}$ is the rate-dependent undrained shear strength and $\sigma_p'^{(d)}$ is the rate-dependent preconsolidation pressure. First, for many commonly used yield surfaces, for example Cam-clay, Modified Cam-clay, and the elliptical cap, there is a fixed ratio between the top of the yield surface (point F in Fig. 1(c)) and the yield surface intercept with the mean stress axis (point B in Fig. 1(c)). Neglecting the effects of strain-hardening before failure or yielding, this ratio is approximately

$$\Lambda = \frac{S_u^{(d)}}{\sigma'^{(d)}_{my}} = \frac{S_u^{(s)}}{\sigma'^{(s)}_{my}} \quad (9)$$

where Λ is a constant governed by the yield surface function and the slope of the critical state line. Substituting equation (9) into equation (8) and modifying the plastic potential for the axial strain during undrained triaxial compression tests gives

$$\log\left(S_u^{(d)}\right) = \alpha \log(\dot{\varepsilon}_a) + \left[\log\left(S_u^{(s)}\right) - \alpha \log\left(\sqrt{\frac{2}{3}}\gamma^{vp}\right)\right] \quad (10)$$

and by similar argument, since $S_u^{(d)}/\sigma_p'^{(d)}$ is also constant giving

$$\log\left(\sigma_p'^{(d)}\right) = \alpha \log(\dot{\varepsilon}_a) + \left[\log\left(\sigma_p'^{(s)}\right) - \alpha \log\left(\sqrt{\frac{3}{5}}\gamma^{vp}\right)\right] \quad (11)$$

Equations (10) and (11) are also straight lines in a log–log plot as shown in Figs 2(b) and 2(c), respectively. Furthermore, equation (11) is similar to the following relationship used by Leroueil & Marques (1996) to characterise the variation of preconsolidation pressure against strain rate in oedometer tests

$$\log(\sigma_p') = \alpha \log(\dot{\varepsilon}_a) + A \quad (12)$$

where α and A are constants.

Referring to Fig. 2(a), a power law flow function implies a linear log–log relation between isotropic yield stress and axial strain rate, which is represented by line A–B in Fig. 2(a). Second, the slope of line A–B, $\alpha = 1/n$, represents the rate-sensitivity of the isotropic yield stress. Third, line A–B terminates at point A, whose coordinates are $\sigma'^{(s)}_{my}$ (the static yield surface) and $\dot{\varepsilon}_a = \gamma^{vp}/3$. Thus, point A in Fig. 1(c) is a static state (i.e. $\sigma'^{(d)}_{my} = \sigma'^{(s)}_{my}$). The value $\dot{\varepsilon}_a = \gamma^{vp}/3$ is a threshold strain rate above which strain rate effects are mobilised. For axial strain rates less than $\gamma^{vp}/3$ the isotropic yield stress is rate-insensitive and the EVP model becomes an elastoplastic model. Conversely, the isotropic yield stress becomes rate-sensitive and the material response is viscous for strain rates exceeding $\gamma^{vp}/3$. Similar principles apply to the preconsolidation pressure and undrained strength, as shown in Fig. 2(b) and 2(c).

In the following sections, equations (8), (10) and (11) are used to evaluate the behaviour of 20 clays during rate-controlled undrained triaxial and oedometer compression tests reported in the literature. Before undertaking such an evaluation, it should be noted that other flow functions have been used in EVP constitutive models (see for example Desai & Zhang, 1987; Katona, 1984; Rocchi *et al.*, 2003). Although this paper focuses exclusively on a power law flow function, a detailed examination of the exponential flow function used by Rocchi *et al.* (2003) can be found in Qu (2008).

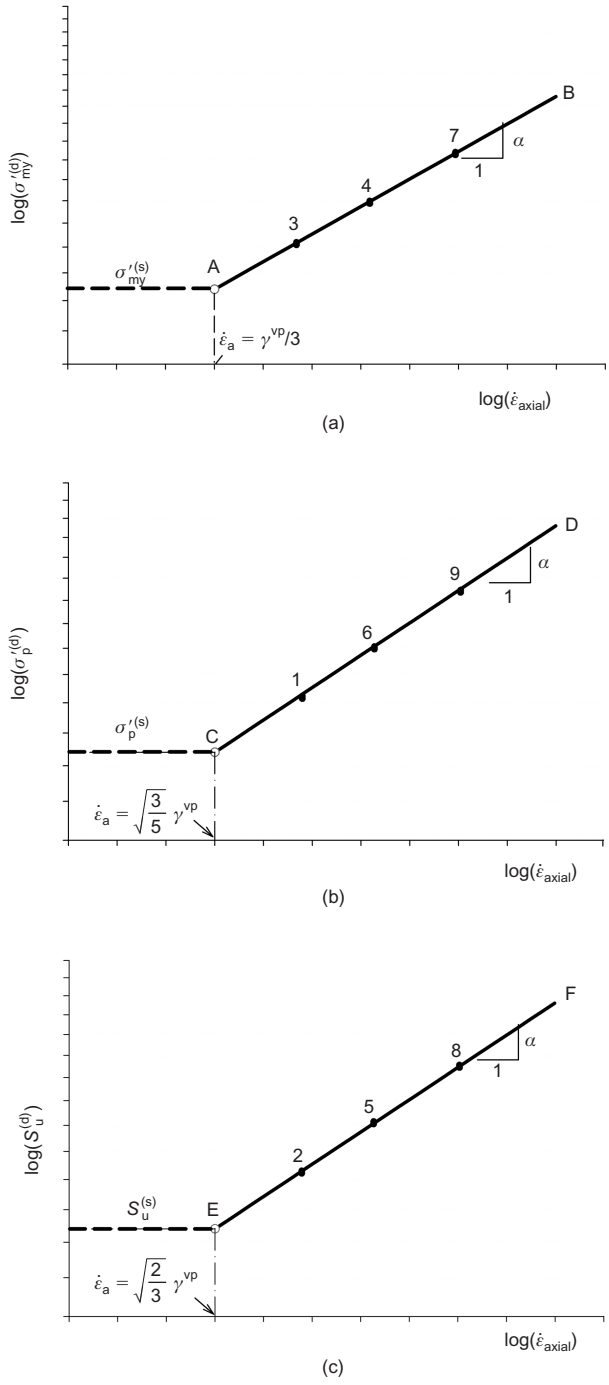

Fig. 2. Variation of $\sigma'^{(d)}_p$, $\sigma'^{(d)}_{my}$ and S_u against axial strain rate during CRS laboratory compression tests (for a power law): (a)–(c) derived from the EVP theory with a power law flow function

Links with the isotache concept

Figure 3 illustrates the main characteristics of a power law EVP model for generalised stresses. In contrast with conventional elastoplastic theory, an EVP model implies a family of dynamic yield surfaces that expand with increasing strain rate, as shown by the dashed lines 1–2–3, 4–5–6 and 7–8–9 in Fig. 3(a). The static yield surface (A–C–E) in Fig. 3(a) defines yield stresses that if exceeded cause viscous behaviour. Lines A–B, C–D, and E–F shown in Fig. 3(a) correspond to those shown in Fig. 2(a), and (b). In addition, lines A–B, C–D and E–F can be linked to each other in general stress space using a suitable yield surface function, $F(\sigma'_{ij},\ \varepsilon^{vp}_{vol})$.

As shown in Fig. 3(b), a series of yield surface isotaches can be constructed by projecting the dynamic yield surfaces in Fig. 3(a) on to the $\sigma'_m - \sqrt{2J_2}$ plane. Each dynamic yield surface defines a locus of rate-dependent yield points in generalised stress space, which is essentially consistent with the isotache concept proposed by Suklje (1957), and extended by Tavenas *et al.* (1978), Graham *et al.* (1983) and Leroueil *et al.* (1985). It can be further deduced that the spacing between yield surface isotaches is governed by α, as shown in Fig. 4. There is, however, one key difference between the isotache concept and generalised EVP theory. In the EVP model, the distribution of dynamic yield surfaces has a lower limit, the static yield surface (ACE), below which the behaviour of clay is elastic and rate-insensitive. In contrast, the isotache concept assumes that isotaches contract infinitely in stress space with the reduction of strain rate. In general, most clays exhibit a unique $\sigma' - \varepsilon - \dot{\varepsilon}$ relationship that is consistent with the EVP theory, however, Sorensen *et al.* (2007) describe clayey soils that do not behave in an isotache manner.

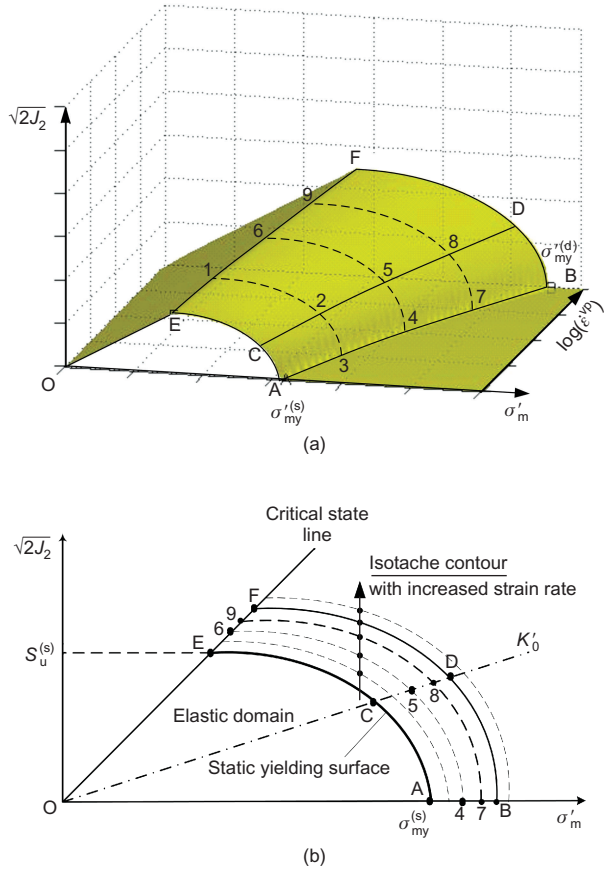

Fig. 3. Characteristics of generalised EVP theory: (a) EVP theory in $\sqrt{2J_2} - \sigma'_m - \log(\dot{\varepsilon}^{vp})$ space; (b) yield surface isotaches

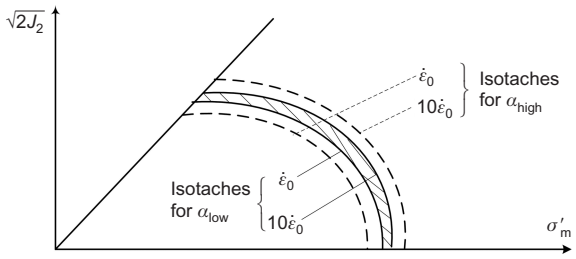

Fig. 4. Influence of α on the spacing of yield surface isotaches

Equations for constant stress tests

Researchers such as Oka *et al.* (1986) and Hinchberger & Rowe (2003) have numerically shown that EVP constitutive models, which use a power law flow functions produce linear variation of void ratio, e, against $\log(t)$ after the end of primary consolidation. Such a relationship can be derived explicitly from equations (3)–(5) as shown below.

First, to simplify the derivation, e_o and $\sigma'^{(s)}_{myo}$ are defined as the void ratio and yield surface intercept at the end of primary consolidation (EOP). Such an assumption removes the need to solve for the viscoplastic strains that occur during primary consolidation. From the flow function (equation (4)) and hardening law (equation (5)) it can be shown that

$$\frac{d\sigma'^{(s)}_{my}}{dt} = \frac{(1+e_o)}{(\lambda-\kappa)}\sigma'^{(s)}_{my}\gamma^{vp}\left(\frac{\sigma'^{(d)}_{my}}{\sigma'^{(s)}_{my}}\right)^n\left[\frac{\partial F}{\partial \sigma'_m}\right] \tag{13}$$

Solving equation (13) gives

$$\frac{1}{n}\left(\sigma'^{(s)}_{my}\right)^n = \frac{(1+e_o)}{(\lambda-\kappa)}\gamma^{vp}\left[\frac{\partial F}{\partial \sigma'_m}\right]\left(\sigma'^{(d)}_{my}\right)^n t + c \tag{14}$$

where t is time after EOP and c is $[\sigma'^{(s)}_{myo}]^n/n$ at $t = 0$. Dividing equation (14) by c and rearranging gives

$$\left(\frac{\sigma'^{(s)}_{my}}{\sigma'^{(s)}_{myo}}\right)^n = n\frac{(1+e_o)}{(\lambda-\kappa)}\gamma^{vp}\left[\frac{\partial F}{\partial \sigma'_m}\right]\left(\frac{\sigma'^{(d)}_{my}}{\sigma'^{(s)}_{myo}}\right)^n t + 1 \tag{15}$$

In EVP theory, secondary compression is attributed to time-dependent plastic strain and thus equation (15) can be reduced further using the hardening law, (e.g. $\Delta e = (e_o - e) = (C_c - C_r)\log[\sigma'^{(s)}_{my}/\sigma'^{(s)}_{myo}]$ and taking the logarithm of equation (15) to give

$$e = e_o - \frac{(C_c - C_r)}{n}\log\left(\frac{t}{\tau} + 1\right) \tag{16}$$

where the parameter

$$\tau = 2{\cdot}3\frac{(C_c - C_r)}{\left[n(1+e_o)\gamma^{vp}[\partial F/\partial \sigma'_m]\left(\frac{\sigma'^{(d)}_{myo}}{\sigma'^{(s)}_{my}}\right)^n\right]}$$

has units of time and can be considered a reference time. Interestingly, equation (16) is similar to the logarithmic creep law used by Leoni *et al.* (2008), who describe in detail how to apply such an equation.

Finally, for normally consolidated clay, and typical values of γ^{vp} and n, it can be shown that $t/\tau + 1 \cong t/\tau$ (see Leoni *et al.*, 2008) and consequently equation (16) defines a linear line in $e-\log(t)$ space with slope $(C_c - C_r)/n$. From classical soil mechanics, the coefficient of secondary compression, $C_{\alpha e}$, is traditionally used to define the variation of void ratio, e, with $\log(t)$ after EOP (see Raymond & Wahls, 1976). Consequently, setting $C_{\alpha e} = (C_c - C_r)/n$ and rearranging gives

$$\alpha = \frac{1}{n} = \frac{C_{\alpha e}}{C_c - C_r} \quad (17)$$

The above derivation shows that the power law exponent, n, in equation (4) can be derived from the coefficient of secondary $C_{\alpha e}$, the isotropic compression index, C_c, and isotropic recompression index, C_r. Thus, if the power law EVP theory is consistent, then α derived from CRSN tests on clay should be consistent with α derived from the response during drained creep. In addition, equation (17) is similar to the equation proposed by Mesri & Choi (1979) and later used by Kim & Leroueil (2001)

$$\alpha = C_{\alpha e}/C_c \quad (18)$$

since C_r is typically small relative to C_c for clays (Holtz & Kovacs, 1981).

EVALUATION

This section examines (a) the influence of strain rate on the preconsolidation pressure of clay during CRSN oedometer compression tests, (b) the influence of strain rate on the undrained shear strength of clay during either CRSN triaxial compression tests or field vane tests, and (c) the secondary compression response of natural and remoulded clays. Table 1 summarises the properties of the clays considered, which originate from Hong Kong, Norway, North Ireland, Britain, Sweden, the United States and Canada. It should be noted that that there have been numerous studies concerning the influence of strain rate on either the undrained shear strength (see Kulhawy & Mayne, 1990) or preconsolidation pressure of clays (e.g. Leroueil & Marques, 1996). For the clays listed in Table 1, however, there is enough experimental data to evaluate the rate-dependent response during drained CRSN oedometer compression, undrained CRSN triaxial compression and secondary compression. Such an evaluation is new.

It is also noted that the data compiled in Table 1 correspond to tests on undisturbed specimens except for: (a) triaxial tests on remoulded Boston blue clay, and (b) oedometer tests (re: secondary compression) on remoulded London clay, Hong Kong clay and San Francisco Bay mud. In addition, since most natural clays are structured to some degree, a few comments on the influence of structure are warranted. First, studies showing the results of CRSN triaxial tests with step-changes in the strain rate performed on undisturbed structured clays indicate that α is the same for both the structured and destructured material (see Hinchberger & Qu, 2007). Consequently, structure is not expected to effect the evaluation of α from CRSN tests, which should be confirmed by the inclusion of data for remoulded clay in the assessment. However, during oedometer tests, destructuration can have a pronounced influence on $C_{\alpha e}$ for stress increments near the preconsolidation pressure. This behaviour may be attributed to changes in the clay fluidity (see Hinchberger & Qu 2009). However, to minimise the effect of structure during oedometer creep compression, the values of $C_{\alpha e}$ reported in Table 2 were obtained from oedometer data corresponding to stress increments much higher than the preconsolidation pressure, where the clay has likely reached or is near to the intrinsic state.

Figure 5 plots $\log(\sigma'_p)$ against $\log(\dot{\varepsilon}_a)$ for 12 of the clays listed in Tables 1 and 2 and reported in the literature. From Fig. 5, it can be seen that the relationship between $\log(\sigma'_p)$ and $\log(\dot{\varepsilon}_a)$ is essentially linear for each clay regardless of the magnitude of preconsolidation pressure (40–1000 kPa) and strain rate (3×10^{-8}/min $- 5{\cdot}0 \times 10^{-3}$/min). As noted in the preceding sections, the effect of strain rate on σ'_p can be represented by α, which has been estimated from the slope of the best-fit line through the data points in Fig. 5 and tabulated in Table 2. For oedometer compression, the slope is denoted by α_{oed}. Referring to Fig. 5 and Table 2, it can be seen that Ottawa clay has the highest rate-sensitivity with $\alpha_{oed} = 0{\cdot}104$ whereas $\alpha_{oed} = 0{\cdot}03$ for Winnipeg clay, which exhibits the lowest rate-sensitivity of the clays examined. Furthermore, it is noted that α_{oed} has generally been measured over three orders of magnitude strain rate for the clays depicted in Fig. 5. The responses of Berthierville and Batiscan clays, however, have been measured over four orders of magnitude change in strain rate.

Table 2. Summary of strain-rate parameters, α

Clay	Reference	α_{uc}	α_{oed}	α_{creep}	α_{avg}
London clay (England)	Lo (1961), Sorensen *et al.* (2007), Gasparre *et al.* (2007)	0·023§	–	0·018	0·021
Remoulded Boston blue clay (USA)	Taylor (1948)	0·024	–	–	0·024
Winnipeg clay (Canada)	Graham *et al.* (1983)	0·031§	0·030†	0·020	0·027
Gloucester clay (Canada)	Law (1974), Lo *et al.* (1976), Leroueil *et al.* (1983)	0·037	0·035	0·043	0·038
Batiscan clay (Canada)	Leroueil *et al.* (1985), Mesri *et al.* (1995)	–	0·047*	0·033	0·040
St Alban clay (Canada)	Tavenas & Leroueil (1978), Tavenas *et al.* (1978)	–	0·039	0·033	0·036
Haney clay (Canada)	Vaid & Campanella (1977a)	0·041	–		0·041
Hong Kong clay	Yin *et al.* (2002)	0·044	–	0·041	0·043
Drammen clay (Norway)	Bjerrum (1967), Berre & Bjerrum (1973)	0·051	0·048†	0·041	0·047
St Jean Vianney clay (Canada)	Vaid *et al.* (1979)	0·045	0·052	–	0·049
Belfast clay (N.Ireland)	Graham *et al.* (1983)	0·046§	0·052	0·056	0·051
Sackville clay (Canada)	Hinchberger (1996), Rowe & Hinchberger (1998).	0·051	–	0·053	0·052
Ska Edeby clay (Sweden)	Wiesel (1973), Mesri *et al.* (1995)	0·055‡	–	0·056	0·055
Backebol clay (Sweden)	Sallfors (1975), Torstensson (1977), Leroueil *et al.* (1985).	0·051‡	0·058	–	0·055
Berthierville clay (Canada)	Leroueil *et al.* (1988), Zhu & Yin (2000), Kim & Leroueil (2001).	–	0·056*	0·057	0·057
St Cesaire clay (Canada)	Leroueil *et al.* (1985)	–	0·067	–	0·067
Louiseville clay (Canada)	Leroueil *et al.* (1985)	–	0·069	–	0·069
San Francisco Bay mud (USA)	Arulanandan *et al.* (1971), Lacerda (1976), Kavazanjian & Mitchell (1980)	0·065		0·077	0·071
Ottawa clay (Canada)	Crawford (1965)	–	0·104	–	0·104
Windsor clay (Canada)	Appendix 2	0·031§	–	0·031	0·031

* From both CRS oedometer and incremental oedometer tests (see Leroueil *et al.* (1988) for interpretation).
† From oedometer tests with 24 h, 7d and 14d load increments (see Graham *et al.* (1983) for interpretation).
‡ From field vane tests performed at different rotation rates (Note: vane results at low strain rates may be influenced by drainage).
§ From CRS triaxial compression tests with step-changes in the strain rate on a single specimen.

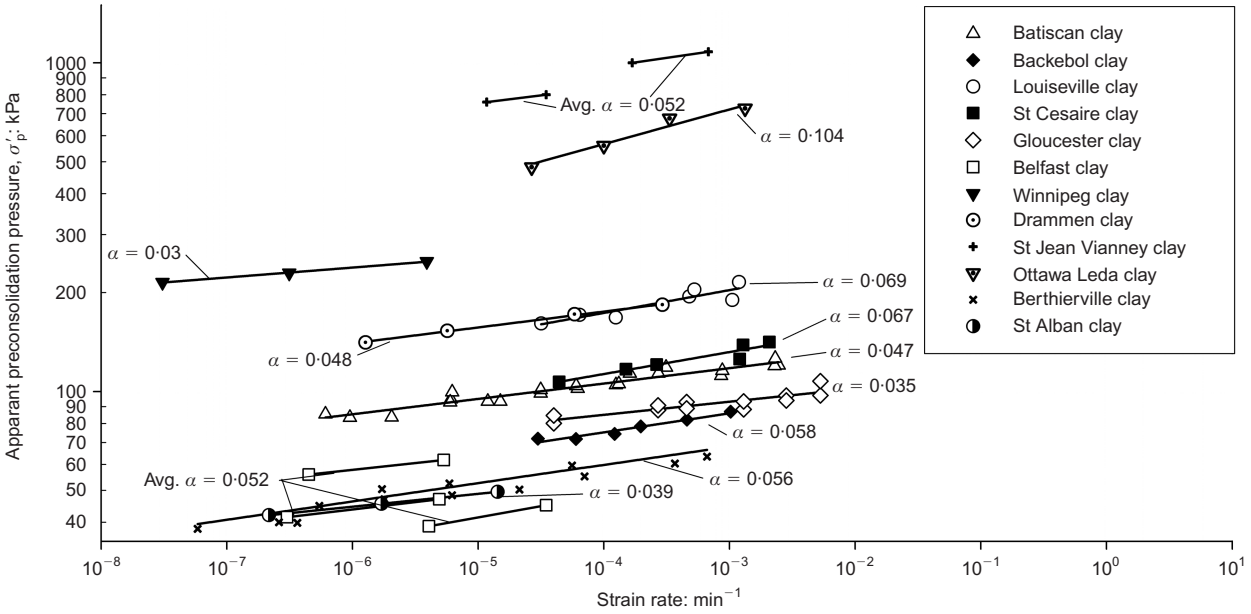

Fig. 5. Measured σ'_p against $\dot{\varepsilon}_{axial}$

Rate-sensitivity of undrained shear strength

In addition to preconsolidation pressure, σ'_p, the undrained shear strength, S_u, of most clays is affected by the strain rate during loading. This observation has been confirmed by numerous studies performed in the laboratory and using field vane tests (e.g. Taylor, 1948; Bjerrum, 1973; Torstensson, 1977; Graham *et al.*, 1983; Kulhawy & Mayne, 1990; and Hinchberger, 1996). In fact, Kulhawy & Mayne (1990) concluded that the average change of S_u is about 10% per log cycle change in strain rate. In this section, the rate-sensitivity of S_u, is characterised by estimating α_{uc}, for 12 of the clays listed in Table 2. In addition, α_{uc} is compared with α_{oed} for the corresponding clay to investigate if α_{uc} and α_{oed} are similar.

For most of the clays reported in Table 2, the influence of $\dot{\varepsilon}_a$ on the undrained strength, S_u, was evaluated using CRSN undrained triaxial compression tests performed on separate samples using different constant rates-of-strain. However, the rate-sensitivity of Windsor, Winnipeg, London and Belfast clays was studied using undrained triaxial compression tests with step-changes in the strain rate. The rate-sensitivity of Backebol clay was studied using field vane tests performed at different rotation rates.

The resultant $\log(S_{uN})$ against $\log(\dot{\varepsilon}_a)$ data for 12 of the clays listed in Table 2 is plotted in Fig. 6, where (S_{uN}) is the normalised undrained shear strength (see Graham *et al.*, 1983). From Fig. 6, it can be seen that $\log(S_{uN})$ against $\log(\dot{\varepsilon}_a)$ is again linear with slope α_{uc} for all of the clays except for Haney clay and Drammen clay, which are plotted separately in Fig. 7. Referring to Fig. 7, the undrained shear strength of Haney clay (Vaid & Campanella, 1977b) is constant when the strain rate is less than 2×10^{-5}/min. Accordingly, for Haney clay, S_u is rate-independent for strain rates less than 2×10^{-5}/min corresponding to the static state (see A in Fig. 2(c)). Similar behaviour is exhibited by

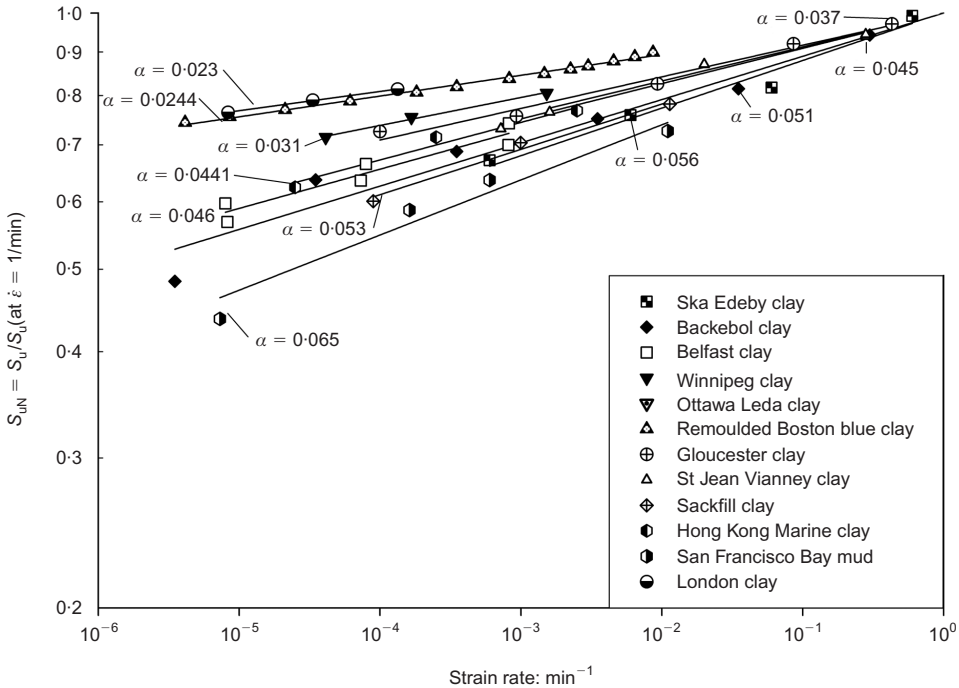

Fig. 6. Undrained shear strength, S_u, against axial strain rate, $\dot{\varepsilon}_{axial}$

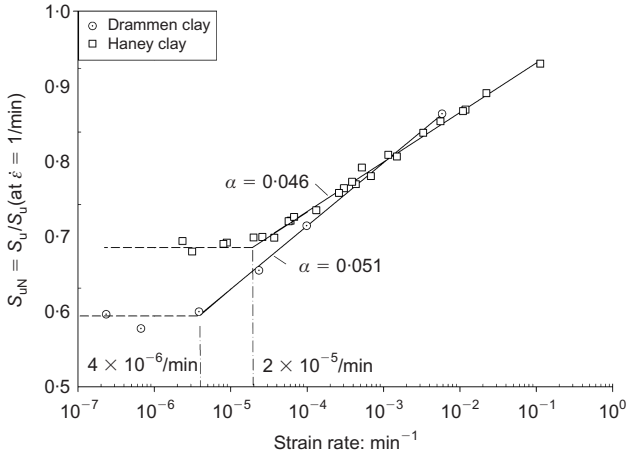

Fig. 7. S_u against $\dot{\varepsilon}_{axial}$ for Drammen clay and Haney clay

Drammen clay (Berre & Bjerrum, 1973) for strain rates of 5×10^{-6}/min or less. However, when the axial strain rate exceeds 2×10^{-5}/min for Haney clay and 5×10^{-6}/min for Drammen clay, the relationship between $\log(S_{uN})$ and $\log(\dot{\varepsilon}_a)$ is essentially linear as seen for the other clays examined in Fig. 6.

Interrelationship between α_{uc} and α_{oed}

From the above data and discussions, α_{uc} and α_{oed} exist for clays from Drammen, Gloucester, Winnipeg, Saint-Jean Vianney, Belfast and Backebol (see Table 2). Consequently, it is possible to use these clays to assess if the rate-sensitivity during undrained triaxial compression is comparable with that during CRSN drained oedometer compression. Accordingly, α_{oed} is plotted against α_{uc} in Fig. 8. In Fig. 8, it can be seen that the rate-sensitivity parameter α_{uc} estimated from $S_u - \dot{\varepsilon}_a$ data is close to α_{oed} from $\sigma'_p - \dot{\varepsilon}_a$. The best agreement between α_{uc} and α_{oed} was found for Winnipeg clay where the difference is only 0·001. In contrast, the poorest agreement is obtained for St Jean Vianney (SJV) clay where the discrepancy is 0·007. For SJV clay, however, the larger discrepancy may be attributed to the natural variability of the clay samples and experimental error due to the triaxial equipment used (see Vaid *et al.*, 1979 and Robertson, 1975). In addition, all data points representing the interrelationship between α_{uc} and α_{oed} fall within the range of ±0·007 from the 1:1 line. Thus, for six clays reported in the literature, the rate-sensitivity parameter, α, measured from CRSN undrained triaxial tests and drained oedometer tests appears to be consistent.

Secondary compression

So far, it has been shown that the rate-sensitivity of the clays presented in Figs 5–7, inclusive, can be quantified by the parameter α. In addition, α appears to be similar for S_u and σ'_p. However, it is not clear if α can be used to characterise other viscous behaviour, such as time-dependent deformation during secondary compression.

In this section, α_{creep}, is estimated from the secondary compression response of 13 clays reported in Table 2 and their corresponding values of C_r, C_c and $C_{\alpha e}$. In most cases, C_r, C_c and $C_{\alpha e}$. were directly reported in the literature as indicated in Table 2. However, for Winnipeg, Batiscan, St. Alban, Belfast and Ska Edeby clays, C_r was not reported. For these cases, C_r was assumed to be $0{\cdot}1C_c$ (see Holtz & Kovacs, 1981). Table 2 summarises the α_{creep} values estimated using equation (16). The published $e-\log(t)$ curves used to determine α_{creep} are summarised in Qu (2008).

Figure 9 shows a plot of α_{creep} and α_{oed} against α_{uc}. Referring to Fig. 9, it can be seen that α_{creep} agrees well with α_{uc}. The best match is found for Sackville clay, where the difference is only 0·0001; whereas the worst match is for San Francisco Bay mud where the discrepancy is 0·012. It should be noted, however, that the laboratory tests utilised to obtain α_{uc} and α_{creep} for San Francisco Bay mud were performed by independent researchers (Lacerda, 1976 and Kavazanjian & Mitchell, 1980) on undisturbed and reconstituted samples, which were also possibly from different depths and locations. In spite of this, the general agreement among α_{creep}, α_{uc} and α_{oed} is encouraging even considering the potential influence of such factors as natural variability, cementation and fabric effects on the laboratory results. Also, the good agreement between α_{creep} and α_{oed} is consistent with Leroueil *et al.* (1985).

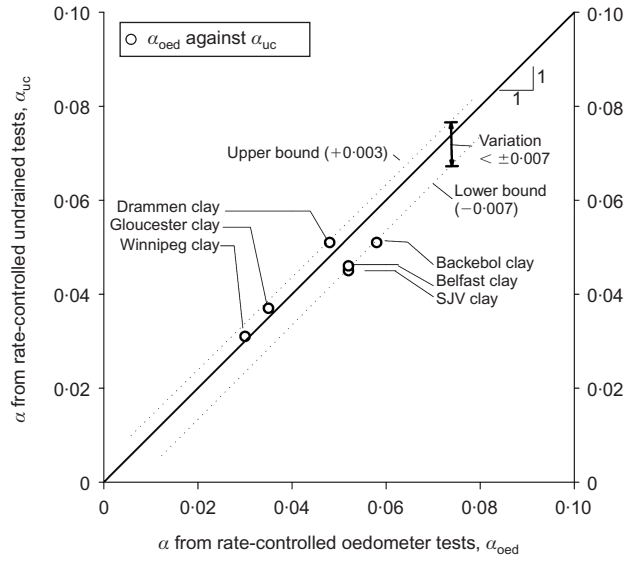

Fig. 8. Comparison of α from rate-controlled oedometer tests and undrained triaxial compression tests (see Table 2)

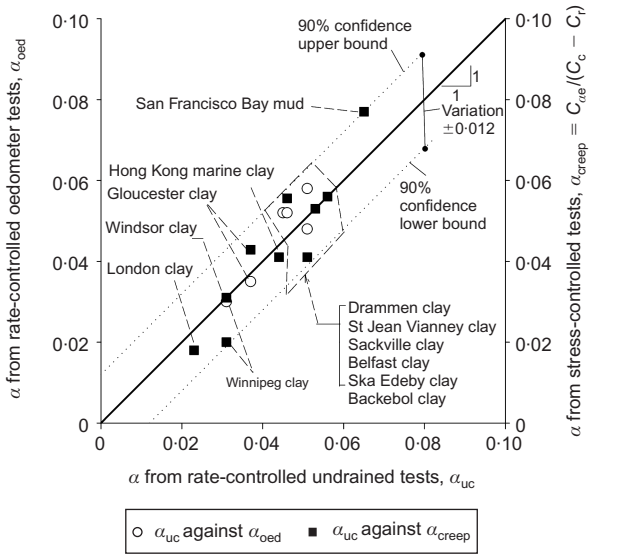

Fig. 9. Comparison of α from secondary consolidation tests, rate-controlled oedometer tests, and undrained triaxial tests (see Table 2)

Discussion

In the preceding sections, the viscous behaviour of 20 clays from Europe to North America was evaluated. From the evaluation, the following main observations can be made.

(*a*) All of the clays examined exhibit an essentially linear log–log relationship between $\sigma'_p - \dot{\varepsilon}_a$, $S_u - \dot{\varepsilon}_a$ and $\sigma'_p - \dot{\varepsilon}_a$ for up to four orders of magnitude change in strain rate. This observation is consistent with equations (10) and (11), which were derived from EVP theory, notwithstanding the limited range of strain rates. Fig. 10, however, summarises σ'_p against $\dot{\varepsilon}_a$ for Gloucester and St Alban clays. In Fig. 10, laboratory measurements of σ'_p have been augmented by in situ estimates of σ'_p obtained from long-term observations of settlements below test embankments (see Leroueil *et al.*, 1983; 1988). The long-term data plotted in Fig. 10 suggest that the linear log-log relation between $\dot{\varepsilon}_a$ and σ'_p may exist over five to six orders of magnitude change in strain rate.

(*b*) For Haney clay and Drammen clay, the linear log–log relationship between $\dot{\varepsilon}_a$ and S_u terminates at a threshold strain rate below which these clays are rate-independent. This is consistent with the concept of a static yield surface.

(*c*) By comparing α_{creep}, α_{uc}, and α_{oed}, the rate-sensitivity parameter, α, appears to be approximately the same for each clay presented in Table 2, regardless of the type of experiment used to measure it. As shown in Fig. 9, the value of α_u from undrained triaxial tests agrees well with α_{oed} and α_{creep} measured from oedometer tests and secondary compression, respectively. Assuming the differences among α_{uc}, α_{creep} and α_{oed} obey a normal distribution, the upper and lower bounds ($\pm 0{\cdot}012$) in Fig. 9 give a visual representation of the 90% confidence for α.

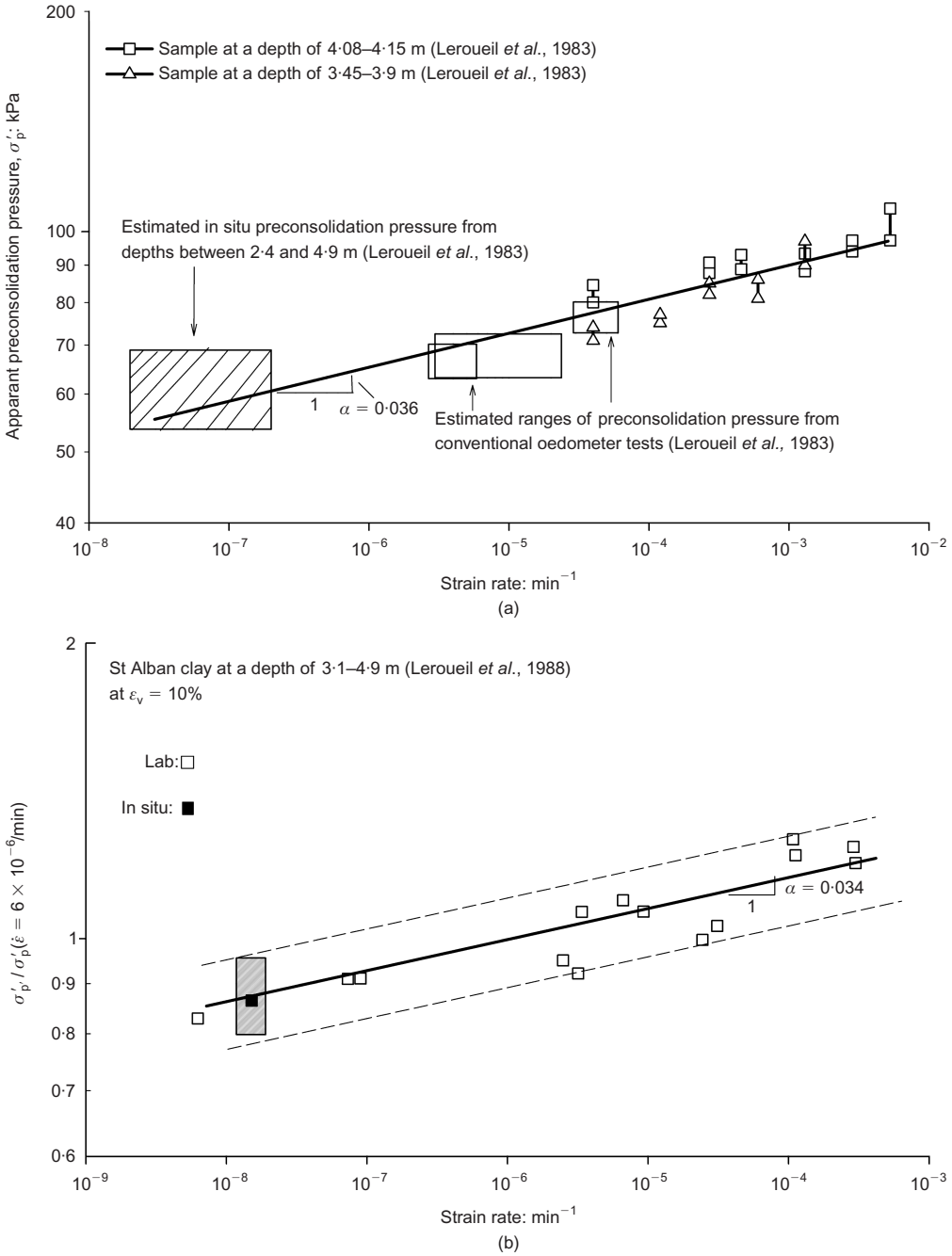

Fig. 10. Combined lab and in situ $\sigma'^{(d)}_p$ for Gloucester clay and St Alban Clay: (a) Gloucester clay (Leroueil *et al.*, 1983); (b) St Alban Clay (Leroueil *et al.*, 1988)

(*d*) From an engineering point of view, it would be desirable to obtain several estimates of α from two or more test methods to determine an average value for use in engineering calculations. Such an evaluation is shown in Fig. 11, which compares α_{uc},, α_{creep} and α_{oed} with the corresponding α_{avg} for each clay listed in Table 2. From this figure, it can be seen that all symbols fall in a narrow range of $\pm 0{\cdot}007$ from the 1:1 line, which is encouraging and suggests that the viscous behaviour of clay in rate-controlled tests and stress-controlled tests is similar and can be characterised simultaneously using the parameter, α.

As shown by Leroueil (2006), the fluidity parameter, γ^{vp} increases with temperature and α is independent of temperature.

SELECTION OF PARAMETERS

One of the main advantages of Perzyna's theory of overstress viscoplasticity (Perzyna, 1963) is that it can be used to extend existing elastoplastic constitutive models to account for the rate-sensitive behaviour of viscous materials. Thus, the parameters of an EVP model can be divided into two groups: (a) elastoplastic and (b) overstress viscoplastic.

Assuming critical state concepts are adopted, then the elastoplastic parameters typically include e, ν, κ, λ, M and a suitable yield function $F(\sigma'_{ij}, \varepsilon_{vol}^{vp})$, where e is the void ratio, ν is Poisson's ratio, κ is the isotropic recompression index, λ is the isotropic virgin compression index, M is the critical state line and ε_{vol}^{vp} is the volumetric plastic strain. Laboratory tests and procedures to obtain these parameters can be readily found in the literature (e.g. Roscoe & Burland, 1968; Chen & Mizuno, 1990; Atkinson, 1993). The yield function, $F(\sigma'_{ij}, \varepsilon_{vol}^{vp})$, links yield points together in generalised stress space corresponding to $S_u^{(d)}$, $\sigma_p'^{(d)}$, and $\sigma_{my}'^{(d)}$ measured at the same strain rate. Thus, a yield surface with an aspect ratio that matches that of the soil must be adopted to simultaneously describe the behaviour of clay over multiple stress paths. The general shape or aspect ratio of the yield surface in compression can be deduced for example from the effective stress path followed during undrained triaxial compression tests on normally consolidated clay (e.g. DeNatale, 1983; Chen & Mizuno, 1990). Alternatively, the yield surface shape can be deduced from a series of drained triaxial stress-path probes (e.g. Tavenas *et al.*, 1978; Leroueil *et al.*, 1979) or from the slope of the critical state line (see Diaz-Rodriguez *et al.*, 1992). Since methods for estimating the elastoplastic parameters in EVP theory are readily available, the following sections deal primarily with the parameters required to define the time-dependency of clay.

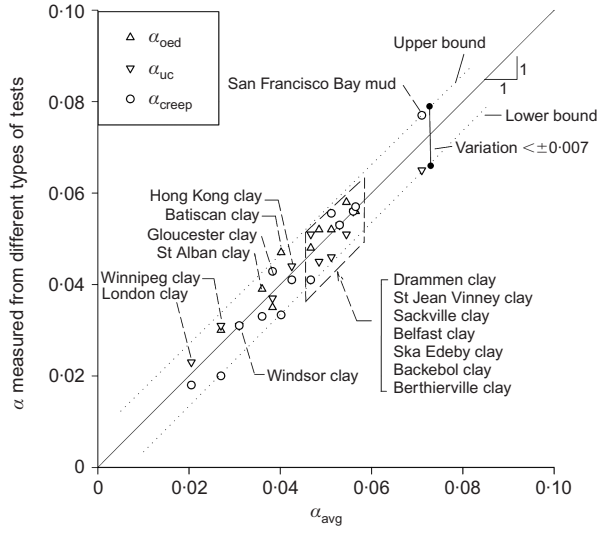

Fig. 11. Comparisons of α_{-uc}, α_{-oed}, and α_{creep} with α_{avg}

Measurement of α

Estimating the strain-rate parameter α is straightforward and can be done in one of two ways: (a) measuring the undrained shear strength against strain rate using CRSN triaxial compression tests and determining the slope of the resultant $\log(S_u) - \log(\dot{\varepsilon}_a)$ response; or (b) measuring the preconsolidation pressure against strain rate using CRSN oedometer compression tests and determining the slope of the resultant $\log(\sigma'_p) - \log(\dot{\varepsilon}_a)$. If either of these two approaches is used, consideration should be given to using tests performed with step-changes in the strain rate to minimise the influence of natural variation (e.g. Richardson & Whitman, 1963; Graham *et al.*, 1983). In addition, the strain rate used in CRSN oedometer tests should be low enough to ensure excess pore pressure dissipation (e.g. Leroueil *et al.*, 1985).

As a check on the value of α measured from CRSN tests, conventional consolidation tests can be performed and α can be deduced from C_r, C_c and $C_{\alpha e}$. Ideally, both CRSN and constant stress tests should be used to determine an average α.

Measurement of $\sigma_{my}'^{(s)}$ and γ^{vp}

$\sigma_{my}'^{(s)}$ and γ^{vp} can be estimated from plots such as that shown in Fig. 2. Depending on the range of strain rates that CRSN tests cover, there are two options available for estimating $\sigma_{my}'^{(s)}$ and γ^{vp}, denoted option 1 and option 2, as described below.

Option 1. For some clays, it is possible to determine the fluidity parameter from the static state. For example, the undrained shear strength of Haney clay (see Fig. 7) is rate-insensitive for strain rates less than or equal to about 2×10^{-5}/min. From Fig. 7, the normalised static shear strength of Haney clay is 0·65, which corresponds to $S_u^{(s)} = 270$ kPa (see Vaid & Campanella, 1977a) and the fluidity parameter is $\gamma^{vp} = \sqrt{3/2} \times 2 \times 10^{-5}/\text{min} \approx 2{\cdot}4 \times 10^{-5}/\text{min}$ (see Fig. 2(c)).

The corresponding static yield surface intercept, $\sigma_{my}'^{(s)}$, can be deduced from the ratio S_u/σ'_{my} for Haney clay using a suitable yield function. If an elliptical cap is used (Chen & Mizuno, 1990), $S_u/\sigma'_{my} = 0{\cdot}49$ can be derived from the slope of the critical state line, $M = 0{\cdot}96$, (see Vaid & Campanella, 1977a) and the aspect ratio of the elliptical cap ($R = 1$, assumed). Consequently, it can be shown that $\sigma_{my}'^{(s)} = 551$ kPa for Haney clay. Appendix 1 summarises the elliptical cap yield function.

Option 1 can also be used if $\sigma'_p - \dot{\varepsilon}_a$ data are available as in the case of Berthierville clay from 3·9–4·8 m depth (Leroueil *et al.*, 1988) as shown in Fig. 12. From Fig. 12, point C corresponds to the static state, which can be reached at axial strain rates less than or equal to about $9 \times 10^{-7}/\text{min}$. As such, the fluidity parameter is $\gamma^{vp} = \sqrt{5/3} \times 9 \times 10^{-7}/\text{min} \cong 1{\cdot}2 \times 10^{-6}/\text{min}$ (see Fig. 2(b)) and the static preconsolidation pressure, $\sigma_p'^{(s)}$, is 80 kPa (from Leroueil *et al.*, 1988). Again, if an elliptical cap (see Appendix 1) is used to model yielding of Berthierville clay, then $\sigma_{my}'^{(s)} = \sigma_p'^{(s)}/1{\cdot}18 = 6{\cdot}78$ kPa, assuming $M = 1$, $R = 0{\cdot}7$ and $K_o' = 0{\cdot}7$.

Option 2. For cases where laboratory testing has not be performed at strain rates low enough to identify a static state

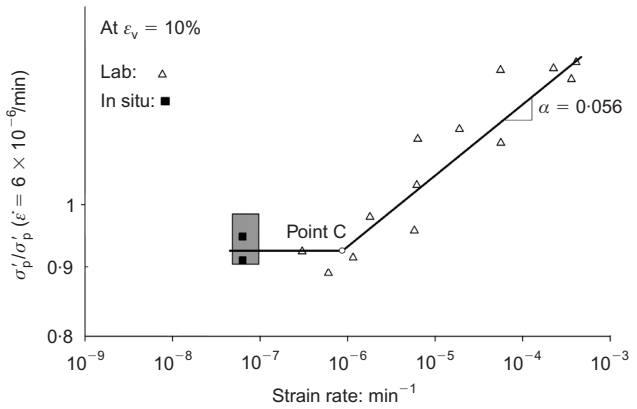

Fig. 12. Normalised $\sigma'_p - \varepsilon$ relationship at 10% vertical strain (ε_v = 10%) for Berthierville clay at a depth of 3·9–4·8 m (data from Leroueil *et al.*, 1988)

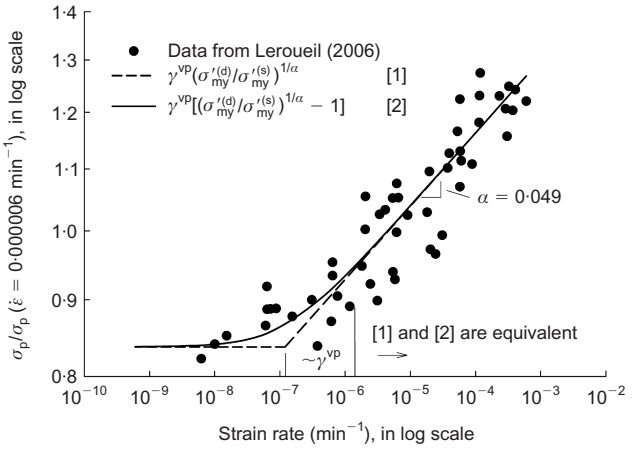

Fig. 13. Data from long-term monitoring of clay (from Leroueil, 2006)

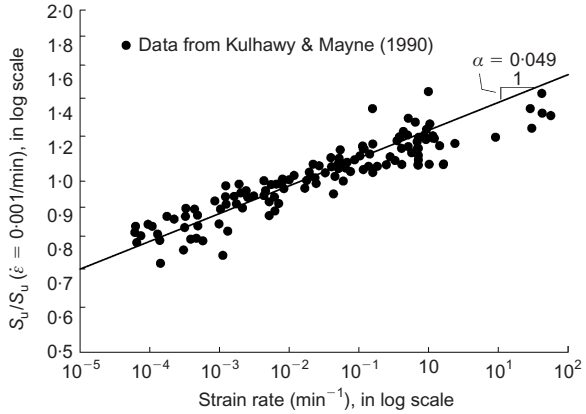

Fig. 14. Comparison of the EVP theory with undrained shear strength against strain rate data from Kulhawy & Mayne (1990)

(e.g. points C or E in Figs 2(b) and 2(c)), the fluidity parameter, γ^{vp}, can be estimated from engineering cases as discussed below.

Figure 10 shows $\log(\sigma'_p) - \log(\dot{\varepsilon}_a)$ data for St. Alban clay and Gloucester clay. As noted above, the data in these figures were obtained using in situ observations of yielding below embankments and using CRSN oedometer tests in the laboratory. For St Alban and Gloucester clays, current observations suggest that the static state has not been reached even at strain rates as low as 6×10^{-9}/min. Consequently, from these cases, a fluidity parameter of 6×10^{-9}/min or lower would be adequate to account for creep strains over the first 25–30 years of service of most engineering structures (see Leroueil *et al.*, 1988 and Hinchberger & Rowe, 1998). From the assumed γ^{vp}, the resultant $\sigma'^{(s)}_{my}$ can be obtained through Figs 2(b) and 2(c) following the same approach illustrated above in option 1.

Discussion

Finally, it is common to use an extended power law function in finite-element implementations of EVP models as follows

$$\phi(F) = \gamma^{vp}\left[\left(\frac{\sigma'^{(d)}_{my}}{\sigma'^{(s)}_{my}}\right)^{n} - 1\right] \tag{19}$$

which is equivalent to the power law flow function, equation (4), except at very low strain rates. Figure 13 compares recent $\sigma'_p - \dot{\varepsilon}_a$ data from Leroueil (2006) with equations (4) and (19) corresponding to $\gamma^{vp} = 1{\cdot}2 \times 10^{-7}$/min and $\alpha = 0{\cdot}049$, which is the average α from the 20 clays summarised in Table 2. From Fig. 13, it can be seen that equations (4) and (19) are equivalent for strain rates exceeding $1{\cdot}2 \times 10^{-7}$/min. As such, the derivations and parameter determination discussed in the preceding sections are also valid for equation (19). However, equation (19) begins to deviate from the power law at strain rates less than about $1{\cdot}4 \times 10^{-6}$/min similar to the long-term data in Fig. 13.

To conclude, Fig. 14 compares the power law with $S_u - \dot{\varepsilon}_a$ data from Kulhawy & Mayne (1990) for 26 different clays. It is interesting that the average value of α from Table 2 ($\alpha = 0{\cdot}049$) also provides a reasonable fit with these data.

SUMMARY AND CONCLUSIONS

This study has evaluated the viscous response of 20 clays reported in the literature using generalised EVP theory. First, theoretical relationships between $S_u - \dot{\varepsilon}_a$, $\sigma'_p - \dot{\varepsilon}_a$, and α and $C_{\alpha e}/(C_c - C_r)$ were derived from EVP theory using a power law flow function. Then, the theoretical relationships were used to examine if the viscous response of clay in compression can be generalised using EVP theory and a single set of viscosity parameters. From this study, the following conclusions can be drawn.

(*a*) All of the clays examined in this paper exhibit linear $\log(S_u) - \log(\dot{\varepsilon}_a)$ and $\log(\sigma'_p) - \log(\dot{\varepsilon}_a)$ responses during both drained and undrained laboratory testing. This is consistent with EVP theory and a power law flow function.

(*b*) This study shows strong evidence that the rate-sensitivity parameter, α, derived from the slope of $\log(S_u) - \log(\dot{\varepsilon}_a)$ and $\log(\sigma'_p) - \log(\dot{\varepsilon}_a)$ plots and from $C_{\alpha e}$, C_r and C_c is consistent even though the stress paths and loading conditions differ in each of these tests.

(*c*) From the data presented in this study, it appears that the viscous response of clay in compression (e.g. S_u against $\dot{\varepsilon}_a$, σ'_p against $\dot{\varepsilon}_a$ and $C_{\alpha e}$) can be fully interpreted using EVP theory in conjunction with a power law flow function provided a suitable yield function, $F(\sigma'_{ij}, \varepsilon^{vp}_{vol})$, is used. For this type of constitutive theory, the viscous constitutive parameters are α, σ'_{my} and γ^{vp}. The yield function links the stress states corresponding to S_u, σ'_p and σ'_{my} measured at the same strain rate together in generalised stress space.

(*d*) The minimum undrained shear strength reached for Haney and Drammen clays (Fig. 7) as well as the

minimum preconsolidation pressure for Berthierville clay (Fig. 12) provide evidence supporting the existence of a static state or a static yield surface for clay (see also Sheahan *et al.*, 1996). The fluidity parameter γ^{vp} from EVP theory can be determined directly from the static state (see Figs 2(b) and 2(c)) and the static yield surface intercept $\sigma'^{(s)}_{my}$ can be deduced directly thereafter from the yield function.

(*e*) In many cases, it may be uneconomic or impractical to establish a static state from laboratory testing. For such cases, it appears to be sufficient to utilise $\gamma^{vp} = 6 \times 10^{-9}$/min, which would cover creep and rate-effects for the first 25–30 years of service life of embankments (see Figs 10 and 13).

ACKNOWLEDGEMENTS

The research presented in this paper was funded by Dr Sean Hinchberger and Dr K. Y. Lo with grants obtained from the National Science and Engineering Research Council of Canada.

APPENDIX 1

The equation of the elliptical yield surface in $\sqrt{2J_2} - \sigma'_m$ stress space is

$$F = (\sigma'_m - l)^2 + 2J_2R^2 - \left(\sigma'^{(s)}_{my} - l\right)^2 = 0$$

where R is the aspect ratio of the elliptical cap, l is the mean effective stress corresponding to the centre of the ellipse, and $\sigma'^{(s)}_{my}$ is the static yield surface intercept (see Chen & Mizuno, 1990).

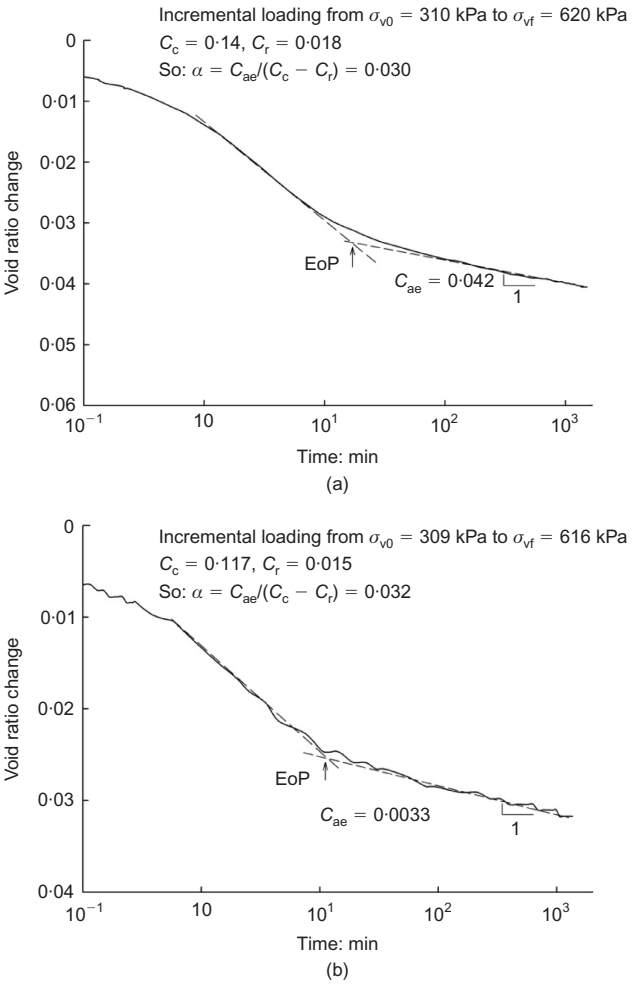

Fig. 15. Typical oedometer increments – Windsor clay: (a) sample 9 BH 14; (b) sample 7 BH 7

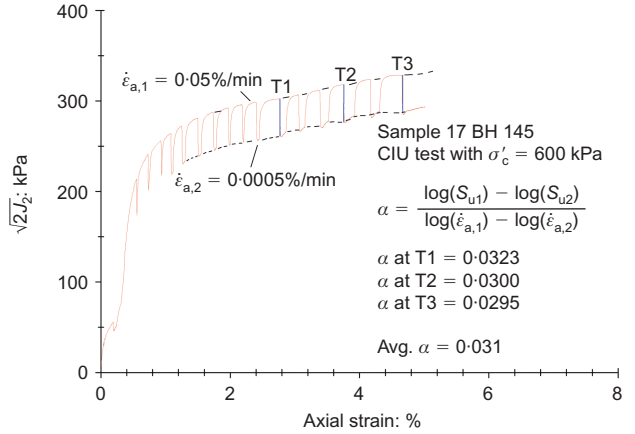

Fig. 16. CRS CIU triaxial test with step-changes in the strain rate – Windsor clay

APPENDIX 2

This appendix summarises the results of two secondary compression tests (see Fig. 15) and one CRSN CIU triaxial test with step-changes in the strain rate (see Fig. 16) that were performed by the authors on clay from Windsor, Ontario, Canada. The specimens were trimmed from Shelby tube samples obtained from 10 m depth. As shown in Figs 15 and 16, the experimental results suggest a consistent rate-sensitivity parameter, α (0·031), can be measured from both time-dependent deformation response and rate effect on CIU test.

REFERENCES

Adachi, T. & Oka, F. (1982). Constitutive equations for normally consolidated clay based on elasto-viscoplasticity. *Soils Found.* **22**, No. 4, 57–70.

Arulanandan, K., Shen, C. K. & Young, R. B. (1971). Undrained creep behaviour of a coastal organic silty clay. *Géotechnique* **21**, No. 4, 359–375, **doi**: 10.1680/geot.1971.21.4.359.

Atkinson, J. H. (1993). *An introduction to the mechanics of soils and foundations: through critical state soil mechanics*. New York: McGraw-Hill.

Berre, T. & Bjerrum, L. (1973). Shear strength of normally consolidated clays. *Proc. 8th Int. Conf. Soil Mech., Moscow*, 39–49.

Bjerrum, L. (1967). Engineering geology of Norwegian normally-consolidated marine clays as related to settlements of buildings. *Géotechnique* **17**, No. 2, 81–118, **doi**: 10.1680/geot.1967.17.2.81.

Bjerrum, L. (1973). Problems of soil mechanics and construction on soft clays. State of the art report. Session IV. *Proc. 8th Int. Conf. Soil Mech., Moscow*, 111–159.

Chen, W. F. & Mizuno, E. (1990). *Nonlinear analysis in soil mechanics: theory and implementation*. New York: Elsevier Science.

Crawford, C. B. (1965). Resistance of soil structure to consolidation. *Can. Geotech. J.* **2**, No. 2, 90–115.

DeNatale, J. S. (1983). *On the calibration of constitutive models by multivariate optimization*. PhD thesis, University of California.

Desai, C. S. & Zhang, D. (1987). Viscoplastic model for geologic materials with generalized flow rule. *Int. J. Numer. Analyt. Methods Geomech.* **11**, No. 6, 603–620.

Diaz-Rodriguez, J. A., Leroueil, S. & Aleman, J. D. (1992). Yielding of Mexico City clay and other natural clays. *J. Geotech. Engng, ASCE* **118**, No. 7, 981–995.

Gasparre, A., Nishimura, S., Coop, M. R. & Jardine, R. J. (2007).

The influence of structure on the behaviour of London Clay. *Géotechnique* **57**, No. 1, 19–31, **doi**: 10.1680/geot.2007.57.1.19.

Graham, J., Crooks, J. H. A. & Bell, A. L. (1983). Time effects on the stress–strain behaviour of natural soft clays. *Géotechnique* **33**, No. 3, 327–340, **doi**: 10.1680/geot.1983.33.3.327.

Hinchberger, S. D. (1996). *The behaviour of reinforced and unreinforced embankments on rate sensitive clayey foundations*. PhD thesis, University of Western Ontario, London.

Hinchberger, S. & Qu, G. (2007). Discussion: Influence of structure on the time-dependent behaviour of a stiff sedimentary clay. *Géotechnique* **57**, No. 9, 783–787, **doi**: 10.1680/geot.2007.57.9.783.

Hinchberger, S. D. & Qu, G. (2009). Viscoplastic constitutive approach for rate-sensitive structured clays. *Can. Geotech. J.* **45**(6): 609–629.

Hinchberger, S. D. & Rowe, R. K. (1998). Modelling the rate-sensitive characteristics of the Gloucester foundation soil. *Can. Geotech. J.* **35**, No. 5, 769–789.

Hinchberger, S. D. & Rowe, R. K. (2003). Geosynthetic reinforced embankments on soft clay foundations: predicting reinforcement strains at failure. *Geotextiles Geomembranes* **21**, No. 3, 151–175.

Holtz, R. D. & Kovacs, W. D. (1981). *An introduction to geotechnical engineering*. Toronto: Prentice Hall.

Katona, M. G. (1984). Evaluation of viscoplastic cap model. *J. Geotech. Engng* **110**, No. 8, 1106–1125.

Kavazanjian, E. & Mitchell, J. (1980). Time-dependent deformation behaviour of clays. *J. Geotech. Engng* **106**, No. 6, 611–630.

Kim, Y. T. & Leroueil, X. (2001). Modeling the viscoplastic behaviour of clays during consolidation: Application to Berthierville clay in both laboratory and field conditions. *Can. Geotech. J.* **38**, No. 3, 484–497.

Kulhawy, F. H. & Mayne, P. W. (1990). *Manual on estimating soil properties for foundation design*. Palo Alto, CA: Electric Power Research Institute.

Lacerda, W. A. (1976). *Stress-relaxation and creep effects on soil deformation*. PhD, University of California, Berkeley, California.

Law, K. T. (1974). *Analysis of embankments on sensitive clays*. PhD thesis, University of Western Ontario, London, Ontario.

Leoni, M., Karstunen, M. & Vermeer, P.A. (2008). Anisotropic creep model for soft soils. *Géotechnique* **58**, No. 3, 215–226, **doi**: 10.1680/geot.2008.58.3.215.

Leroueil, S. (2006). The isotache approach. Where are we 50 years after its development by Professor Suklje. *Proc. 13th Danube Eur. Conf. Geotech. Engng, Ljubljana* **1**, 55–88.

Leroueil, S. & Marques, M. E. S. (1996). Importance of strain rate and temperature effects in geotechnical engineering. *Measuring and modeling time dependent soil behaviour*, Geotechnical special publication No. 61 (eds T. C. Sheahan and V. N. Kaliakin), pp. 1–60. Washington D.C.: ASCE.

Leroueil, S., Tavenas, F., Brucy, F., La Rochelle, P. & Roy, M. (1979). Behavior of destructured natural clays. *J. Geotech. Engng Div.* **105**, No. 6, 759–778.

Leroueil, S., Samson, L. & Bozozuk, M. (1983). Laboratory and field determination of preconsolidation pressures at Gloucester. *Can. Geotech. J.* **20**, No. 3, 477–490.

Leroueil, S., Kabbaj, M., Tavenas, F. & Bouchard, R. (1985). Stress–strain–strain rate relation for the compressibility of sensitive natural clays. *Géotechnique* **35**, No. 2, 159–180, **doi**: 10.1680/geot.1985.35.2.159.

Leroueil, S., Kabbaj, M. & Tavenas, F. (1988). Study of the validity of a σ'–ε_v–$\dot{\varepsilon}$ rate model in in situ conditions. *Soils Found*. **28**, No. 3, 13–25.

Lo, K. Y. (1961). Secondary compression of clays. *J. Geotech. Geoenviron. Engng* **87**, No. 4, 61–87.

Lo, K. Y., Bozozuk, M. & Law, K. T. (1976). Settlement analysis of the Gloucester test fill. *Can. Geotech. J.* **13**, No. 4, 339–354.

Mesri, G. & Choi, Y. K. (1979). Discussion on 'Strain rate behaviour of St. Jean Vianney clay'. *Can. Geotech. J.* **16**, No. 4, 831–834.

Mesri, G., Feng, T. W. & Shahien, M. (1995). Compressibility parameters during primary consolidation. *Proceedings of international symposium on compression and consolidation of clayey soils*, Hiroshima, Japan, pp. 1021–1037.

Norton, F. H. (1929). *The creep of steel at high temperature*. New York: McGraw-Hill.

Oka, F., Adachi, T. & Okano, Y. (1986). Two-dimensional consolidation analysis using an elasto-viscoplastic constitutive equation. *Int. J. Numer. Analyt. Methods Geomech.* **10**, No. 1, 1–16.

Perzyna, P. (1963). Constitutive equations for rate sensitive plastic materials. *Q. Appl. Math*. **20**, No. 4, 321–332.

Qu, G. (2008). *Selected issues on the performance of embankments on clay foundations*. PhD thesis, the University of Western Ontario, London, Canada.

Raymond, G. P. & Wahls, H. E. (1976). *Special report: estimating 1-dimensional consolidation, including secondary compression, of clay loaded from overconsolidated to normally consolidated state*. Washington, DC: National Research Council, Transportation Research Board.

Richardson, A. M. & Whitman, R. V. (1963). Effect of strain-rate upon undrained shear resistance of saturated remoulded fat clay. *Géotechnique* **13**, No. 4, 310–324, **doi**: 10.1680/geot.1963.13.4.301.

Robertson, P. K. (1975). *Strain rate behaviour of Saint-Jean-Vianney clay*. PhD thesis, University of British Columbia, British Columbia, Canada.

Rocchi, G., Fontana, M. & Da Prat, M. (2003). Modelling of natural soft clay destruction processes using viscoplasticity theory. *Géotechnique* **53**, No. 8, 729–745, **doi**: 10.1680/geot.2003.53.8.729.

Roscoe, K. H. & Burland, J. B. (1968). *On the generalised stress–strain behaviour of wet clay*. Cambridge: Cambridge University Press.

Rowe, R. K. & Hinchberger, S. D. (1998). The significance of rate effects in modelling the Sackville test embankment. *Can. Geotech. J.* **35**, No. 3, 500–516.

Sallfors, G. (1975). *Preconsolidation pressure of soft high plastic clays*. PhD thesis, Chalmers University of Technology, Gothenburg, Sweden.

Sheahan, T. C., Ladd, C. C. & Germaine, J. T. (1996). Rate-dependent undrained shear behavior of saturated clay. *J. Geotech. Engng* **122**, No. 2, 99–108.

Sorensen, K. K., Baudet, B. A. & Simpson, B. (2007). Influence of structure on the time-dependent behaviour of a stiff sedimentary clay. *Géotechnique* **57**, No. 1, 113–124, **doi**: 10.1680/geot.2007.57.1.113.

Suklje, L. (1957). The analysis of the consolidation process by the isotache method. *Proc. 4th Int. Conf. Soil Mech. Found. Engng, London*, 319–326.

Tavenas, F. & Leroueil, S. (1978). Effects of stresses and time on yielding of clays. *Proc. 9th Int. Conf. Soil Mech. Found. Engng, Tokyo*, 319–326.

Tavenas, F., Leroueil, S., La Rochelle, P. & Roy, M. (1978). Creep behaviour of an undisturbed lightly overconsolidated clay. *Can. Geotech. J.* **15**, No. 3, 402–423.

Taylor, D. W. (1948). *Fundamentals of soil mechanics*. New York: John Wiley.

Torstensson, B. A. (1977). Time-dependent effects in the field vane test. *International Symposium on Soft Clays*, Bangkok, pp. 387–397.

Vaid, Y. P. & Campanella, R. G. (1977a). *Time-dependent behavior of an undisturbed clay*. Report, University of British Columbia, Vancouver.

Vaid, Y. P. & Campanella, R. G. (1977b). Time-dependent behavior of undisturbed clay. *J. Geotech. Engng Div.* **103**, No. 7, 693–709.

Vaid, Y. P., Robertson, P. K. & Campanella, R. G. (1979). Strain rate behaviour of Saint-Jean-Vianney clay. *Can. Geotech. J.* **16**, No. 1, 35–42.

Wiesel, C. E. (1973). Some factors influencing in situ vane test results. *Proc. 8th ICSMFE, Moscow*, 475–479.

Yin, J.-H., Zhu, J.-G. & Graham, J. (2002). A new elastic viscoplastic model for time-dependent behaviour of normally and over-consolidated clays: theory and verification. *Can. Geotech. J.* **39**, No. 1, 157–173.

Zhu, G. & Yin, J.-H. (2000). Elastic visco-plastic consolidation modelling of clay foundation at Berthierville test embankment. *Int. J. Numer. Analyt. Methods Geomech*. **24**, No. 5, 491–508.